Electronic Supplementary Information (ESI)

Superstructured metallocorroles for electrochemical CO_2 reduction

Woormileela Sinha,[a] Atif Mahammed,[a] Natalia Fridman,[a] Yael Diskin-Posner,[b] Linda J. W. Shimon[b] and Zeev Gross*[a]

[a.] *Schulich Faculty of Chemistry, Technion-Israel Institute of Technology, Haifa, Israel 3200003.*
[b.] *Department of Chemical Research Support, Weizmann Institute of Science, Rehovot, 76100, Israel.*

List of Figures Page No.

List of tables

Materials and Methods

Cobalt(II) acetate tetrahydrate and iron(II) chloride tetrahydrate were purchased from Alfa Aesar and Merck respectively. Tetrabutylammonium perchlorate (TBAP), ferrocene and anhydrous dichloromethane (DCM) were purchased from Sigma Aldrich. All other solvents used for electrochemical and spectroscopic measurements were of HPLC grade.

High-resolution mass (HRMS) spectra were recorded on a Bruker MaXis Impact mass spectrometer. A Cary 8454 UV-Vis spectrometer by Agilent Technologies was used to measure the UV-Vis spectra of the compounds.

^{1}H NMR spectra were recorded on Bruker Avance III 400, Bruker Avance 500, Bruker Avance 600 spectrometers operating at 400.4 MHz, 500.13 MHz and 600.5 MHz respectively. ^{19}F NMR spectra were measured on Bruker Avance III 400 and Bruker Avance 600 spectrometers operating at 376.7 MHz and 565 MHz respectively. Chemical shifts are reported in ppm with respect to the signals from the residual hydrogen atoms in the deuterated solvents, $CDCl_3$ and Pyridine-d_5.

Electrochemical measurements were performed on a 3-electrode system using EMStat3 + electrochemical system and the glassy carbon (working electrode), Ag/AgCl (reference electrode) and platinum wire (counter electrode). 0.5 mM catalyst was used in the presence of 0.1 M TBAP (supporting electrolyte) with scan rate of 100 mV/s. The redox potentials of the complexes are reported with respect to ferrocene/ ferrocenium (Fc/Fc^+) couple. The redox potential of Fc/Fc^+ in acetonitrile was measured to be 0.45 V. For bulk electrolysis measurements, ~ 0.04 mM acetonitrile solutions of catalysts with 0.1 M TBAP were subjected to a constant potential of -1.8 V (vs. Ag/AgCl) in an air-tight electrolytic cell, using a porous carbon electrode (working electrode) and a platinum coil compartmentalized inside a glass tube with a porous fret (counter lectrode). The electrolytic solution was purged with CO_2 for 20 min before doing chronoamperometric measurements.

HPLC analysis was done in a Jasco HPLC instrument using a MD-4010 PDA detector, AS-4050 autosampler, PU-4180 pump. Flow rate was maintained at 4 mL/ min using acetonitrile as the eluent through a LiChrospher RP18-5 Endcapped column (Length X i. d. 25 cm X 4.6 mm).

Gas Chromatographic analysis for the detection of gases evolved during the electrocatalytic reduction of CO_2 was done using a 4210 GC System from Sion Industries with a TCD (thermal

conductivity detector). The amount of CO generated was quantified by its response in a HP-MOLESIEVE column and helium as the carrier gas. The overhead gas inside the cell was taken out with the help of a 1000 μL air-tight syringe (degassed beforehand with CO_2 several times). The oven temperature was maintained at 40° C and the retention time of CO was 11 min. The amount of CO evolved was quantified by calibrating against known volumes of pure CO.

For 1-Co(PPh$_3$): Single crystals of **1-Co(PPh$_3$)** were dipped in Paratone-N oil and quickly mounted on a Kappa CCD diffractometer in the presence of a stream of nitrogen at 200 K. Data collection was done with monochromatic Mo Kα radiation using φ and ω scans to cover the Ewald sphere.[1] Accurate cell parameters were acquired with complete collections of intensities, and were corrected in the usual way.[2] Using Olex2,[3] the structure was solved with the SIR2004[4] structure solution program using Direct Methods and refined with the Shelxl[5] refinement package using Least Squares minimization. Hydrogen atoms were calculated using the riding model. All non-hydrogen atoms were refined with anisotropic displacement parameters.

For 1-Fe(NO): Single crystals of **1-Fe(NO)** were diffracted by a Rigaku XtaLab Pro diffractometer, CuKα (λ=1.54184Å) equipped with PILATUS 200 detector, $-9\leq h\leq 9$, $-48\leq k\leq 48$, $-13\leq l\leq 13$, frame scan width = 0.5°, scan speed 1.0° per 40 sec for low resolution and 200 sec for high resolution, 27760 reflections collected, 11257 independent reflections (R-int =0.0557). The data were processed with CrysAlis[6]. Structure solved with SHELXT[7]. Full matrix least-squares refinement based on F^2 with SHELXL[5] on 1158 parameters with 8 restraints gave final R_1= 0.0528 (based on F^2) and wR_2=0.1378 for data with $I>2\sigma(I)$ and, R_1= 0.0605 and wR_2=0.1434 on 11257 reflections, goodness-of-fit on F^2 = 1.083 largest electron density peak 0.497 $e\cdot Å^{-3}$. Largest hole – 0.654 $e\cdot Å^{-3}$. The structure of **1-Fe(NO)** has a disorder of the nitrosyl iron with ratios 87:13 and 68:32. Four fluorine atoms are also disordered in the crystal.

Synthesis and Characterization

10-(4,7-Dimethoxynaphthalen-1-yl)-5,15-bis(petafluorophenyl)corrolato-cobalt(III)-triphenylphosphine, 1-Co(PPh$_3$)

1-Co(PPh$_3$) was prepared and purified by following a previous report.[8] Recrystallization from a mixture of DCM and hexane afforded pure crystals of the complex (26 mg, 94 % yield). UV-Vis (toluene): $\lambda_{max}(\varepsilon \times 10^4)$ 379 nm (4.45), 413 nm (4.65), 559 nm (1.10), 591 nm (0.95). HRMS (APCI negative mode) for $C_{43}H_{19}CoF_{10}N_4O_2$ *m/z* = 872.0660 (measured, 100 %, $[M - PPh_3]^-$), 872.0686 (calculated) [Figure S1]. ^{1}H NMR (300 MHz, $CDCl_3$) δ 8.70 (d, *J* = 4.5 Hz), 8.46 (d, *J* = 4.5 Hz), 8.44– 8.31 (m), 8.21– 8.15 (m), 8.12 (dd, *J* = 4.8, 1.2 Hz), 8.05 (d, *J* = 4.8 Hz), 8.01 (d, *J* = 4.5 Hz), 7.94 (d, *J* = 4.2 Hz), 7.79 (d, *J* = 7.9 Hz), 7.14– 6.89 (m), 6.79 – 6.60 (m), 6.49 (d, *J* = 2.5 Hz), 4.86 – 4.64 (m), 4.20 (s), 2.87 (s), 2.26 (s) [Figure S2]. ^{19}F NMR (377 MHz, $CDCl_3$) δ -136.92– -137.09 (m), -137.85 – -138.12 (m), -154.09– -154.233 (m), -161.97 – -162.12 (m), -162.50 – -162.65 (m) [Figure S3].

10-(4,7-Dimethoxynaphthalen-1-yl)-5,15-bis(petafluorophenyl)corrolato-cobalt(III)*bis*-pyridine, 1-Co(Py)$_2$

1-Co(Py)$_2$ was also synthesized and purified following the previous report.[8] Recrystallization in a solvent mixture of DCM and hexane in the presence of a few drops of pyridine afforded pure compound (20 mg, 80 % yield). UV-Vis (toluene-0.1% pyridine): $\lambda_{max}(\varepsilon \times 10^4)$ 438 nm (7.94), 586 nm (2.21), 611 nm (3.48) HRMS (APCI negative mode) for $C_{43}H_{19}CoF_{10}N_4O_2$ *m/z* = 872.0625 (measured, 100 %, $[M - Py_2]^-$), 872.0686 (calculated) [Figure S5]. ^{1}H NMR (400 MHz, $CDCl_3$) δ 9.14 (d, *J* = 4.2 Hz, 2H), 8.75 (d, *J* = 4.5 Hz, 2H), 8.65 (broad s, 2H), 8.53 (d, *J* = 4.2 Hz, 2H), 8.36 (d, *J* = 9.3 Hz, 1H), 8.04 (d, *J* = 7.8 Hz, 1H), 7.02 (d, *J* = 7.8 Hz, 1H), 6.98 (dd, *J* = 9.3, 2.5 Hz, 1H), 5.98 (s, 2H, *para*-H of pyridine), 5.69 (s, 1H), 5.07 (s, 4H, *meta*-H of pyridine), 4.22 (s, 3H), 2.20 (s, 3H) [Figure S6]. ^{19}F NMR (377 MHz, $CDCl_3$) δ -138.07 – -138.46 (m, 4F), -154.59 (t, *J* = 22.0 Hz, 2F), -162.69– -162.90 (m, 4F) [Figure S7].

10-(4,7-Dimethoxynaphthalen-1-yl)-5,15-bis(petafluorophenyl)corrolato-iron(III)-nitrosyl, 1-Fe(NO)

1-Fe(NO) was prepared by previously reported protocols.[9] After evaporation of the solvents from the reaction mixture, the crude product was dissolved in DCM to prepare a silica gel slurry and

further subjected to a column chromatographic purification. By a solvent mixture containing 30 % DCM-hexane, the red colored compound was isolated (25 mg, 45 % yield). Further recrystallization using DCM-hexane afforded pure crystalline material in UV-Vis (toluene): λ_{max}($\varepsilon \times 10^4$) 380 nm (7.06), 551 nm (1.50). HRMS (APCI negative mode) for $C_{43}H_{19}F_{10}FeN_4O_2$ *m/z* = 869.0679 (measured, 100 %, $[M\text{-}NO]^-$), 869.0703 (calculated) [Figure S8]. ^{1}H NMR (400 MHz, $CDCl_3$) δ 8.33 (d, *J* = 3.7 Hz), 8.30 (d, *J* = 3.6 Hz), 8.10 (d, *J* = 4.7 Hz), 8.05 (d, *J* = 4.7 Hz), 7.72 – 7.61 (m), 7.32-7.31 (m), 7.15 (dd, *J* = 9.3, 2.5 Hz), 7.11 (dd, *J* = 9.3, 2.5 Hz), 6.91– 6.87 (m), 6.77 (d, *J* = 2.4 Hz), 6.66 (d, *J* = 2.4 Hz), 4.14 (s), 4.13 (s), 3.49 (s), 3.31 (s) [Figure S9]. ^{19}F NMR (377 MHz, $CDCl_3$) δ -137.17 – -137.38 (m, 4F), -152.20– -152.32 (overlapping triplets, 2F), -160.62 – -160.80 (m, 4F) [Figure S10].

10-(4,7-Dihydroxynaphthalen-1-yl)-5,15-bis(petafluorophenyl)corrole, 2

A 5 mL anhydrous DCM solution of BBr_3 (926 μL, 9.76 mmol) was added dropwise into a 10 mL DCM solution of **1** (100 mg, 0.12 mmol) under inert conditions at 0 °C. After completion of addition, the reaction was kept stirring for 24 hours at room temperature. At the end of the reaction, the reaction was washed using a saturated solution of $NaHCO_3$ and then twice with water. Finally, after drying over anhydrous Na_2SO_4, the solvent was evaporated, and the product was purified by a column chromatography using silica gel and 100 % DCM as eluent. Pure crystalline product was obtained by recrystallization from DCM and hexane (160 mg, 83 % yield). UV-Vis (toluene): λ_{max} ($\varepsilon \times 10^4$) 424 nm (9.68), 562 nm (1.65), 616 nm (0.99), 640 nm (0.68). HRMS (APCI negative mode) for $C_{41}H_{17}F_{10}N_4O_2$ *m/z* = 787.1205 (measured, 100 %, $[M\text{-}H]^-$), 787.1197 (calculated) [Figure S12]. ^{1}H NMR (300 MHz, $CDCl_3$) δ 9.10 (d, *J* = 4.3 Hz, 2H), 8.57 (m, 4H), 8.41 (d, *J* = 4.7 Hz, 2H), 8.16 (d, *J* = 9.1 Hz, 1H), 7.85 (d, *J* = 7.6 Hz, 1H), 7.00 (dd, *J* = 9.1, 2.1 Hz, 1H), 6.80 (d, *J* = 7.6 Hz, 1H), 6.27 (d, *J* = 2.1 Hz, 1H) [Figure S13]. ^{19}F NMR (565 MHz, $CDCl_3$) δ -133.83 (ddd, *J* = 31.4, 23.8, 6.9 Hz, 4F), -148.75 (t, *J* = 20.8 Hz, 2F), -157.69– -157.76 (m, 4F) [Figure S14].

10-(4,7-Dihydroxynaphthalen-1-yl)-5,15-bis(petafluorophenyl)corrolato-cobalt(III)*bis*-pyridine, 2-Co(Py)$_2$

2-Co(Py)$_2$ was prepared in a similar way as **1-Co(Py)$_2$** was prepared. The green colored reaction crude was purified using silica-gel column and DCM:hexane:pyridine (4:1:0.01 ratio) as eluent and obtained (19 mg, 75% yield). UV-Vis (toluene-0.1% pyridine): λ_{max} ($\varepsilon \times 10^4$) 438 nm (6.20),

588 nm (1.79), 612 nm (2.48). HRMS (APCI negative mode) for $C_{41}H_{15}CoF_{10}N_4O_2$ *m/z* = 844.0388 (measured, 100 %, $[M\text{-}Py_2]^-$), 844.0373 (calculated) [Figure S15]. ^{1}H NMR (500 MHz, Pyridine-d_5) δ 9.59 (d, *J* = 4.2 Hz, 2H), 9.35 (d, *J* = 4.6 Hz, 2H), 9.21 (d, *J* = 4.3 Hz, 4H), 9.06 (d, *J* = 9.1 Hz, 1H), 8.15 (d, *J* = 7.6 Hz, 1H), 7.55 (d, *J* = 9.1 Hz, 1H), 7.43 (d, *J* = 7.5 Hz, 1H), 6.66 (s, 1H) [Figure S16]. ^{19}F NMR (188 MHz, Pyridine-d_5) -138.85 (ddd, *J* = 54.6, 25.9, 8.1 Hz, 4F), -155.14 (t, *J* = 21.7 Hz, 2F), -163.20 (ddd, *J* = 47.5, 25.6, 8.3 Hz, 4F) [Figure S17].

10-(4,7-Di-*tert*-butyldimethylsilyl-naphthalen-1-yl)-5,15-*bis*(petafluorophenyl)corrole, 3

To a vial containing 1 mL of anhydrous DCM solution of free-base corrole **2** (20 mg, 0.025 mmol) and imidazole (8.5 mg, 0.125 mmol), tert-butyldimethylsilyl chloride (18.8 mg, 0.125 mmol) was added and the reaction was stirred overnight under inert atmosphere. At the completion of the reaction, the reaction mixture was washed with water and dried over anhydrous Na_2SO_4. The solvent was evaporated and the crude product after chromatographic separation on a silica gel column using 15% DCM-hexane as eluent afforded the desired compound **3** (20 mg, 78 % yield). UV-Vis (toluene): λ_{max} (Ɛ × 10^4) 424 nm (8.58), 568 nm (1.69), 618 nm (1.14), 640 nm (0.86). HRMS (APCI negative mode) for $C_{53}H_{45}F_{10}N_4O_2Si_2$ *m/z* = 1015.2898 (measured, 100 %, $[M\text{-}H]^-$), 1015.2927 (calculated) [Figure S18]. ^{1}H NMR (500 MHz, $CDCl_3$) δ 9.11 (d, *J* = 3.0 Hz, 2H), 8.61 (s, 2H), 8.57 (s, 2H), 8.50 (d, *J* = 3.8 Hz, 2H), 8.39 (d, *J* = 9.1 Hz, 1H), 7.96 (d, *J* = 7.5 Hz, 1H), 7.11 (d, *J* = 7.0 Hz, 2H), 6.56 (s, 1H), 1.26 (s, 9H), 0.54 (s, 6H), 0.53 (s, 9H), -0.48 (s, 6H) [Figure S19]. ^{19}F NMR (377 MHz, $CDCl_3$) δ -137.77 – -137.99 (m), -152.92 (t, *J* = 20.5 Hz), -161.70 – -161.95 (m) [Figure S20].

10-(4,7-Di-*tert*-butyldimethylsilyl-naphthalen-1-yl)-5,15-bis(petafluorophenyl)corrolato-cobalt(III)*bis*-pyridine, 3-Co(py)$_2$

3-Co(py)$_2$ was prepared in a similar protocol as discussed for the synthesis of **1-Co(py)$_2$** and **2-Co(py)$_2$**. The crude product was purified by column chromatography using silica gel column and DCM:hexane:pyridine (1:6:0.01) to get the pure form of **3-Co(py)$_2$** (18 mg, 75 % yield). UV-Vis (toluene-0.1% pyridine): λ_{max} (Ɛ × 10^4) 439 nm (7.60), 587 nm (2.05), 612 nm (3.26). HRMS (APCI negative mode) for $C_{53}H_{43}CoF_{10}N_4O_2Si_2$ *m/z* = 1072.2109 (measured, 100 %, $[M\text{-}Py_2]^-$), 1072.2091 (calculated) [Figure S21]. ^{1}H NMR (500 MHz, Pyridine-d_5) δ 9.56 (d, *J* = 4.2 Hz, 2H), 9.38 (d, *J* = 4.5 Hz, 2H), 9.24 (d, *J* = 4.1 Hz, 2H), 9.07 (d, *J* = 4.7 Hz, 2H), 8.08 (d, *J* = 7.7 Hz, 1H), 7.37 (dd, *J* = 9.2, 2.2 Hz, 1H), 7.25 (d, *J* = 7.7 Hz, 1H), 6.88 (d, *J* = 2.1 Hz, 1H), 1.22 (s, 9H),

0.59 (s, 9H), 0.49 (s, 6H), -0.35 (s, 6H) [Figure S22]. ^{19}F NMR (377 MHz, Pyridine-d_5) δ -138.86 – -139.13 (m), -155.15 (t, J = 21.4 Hz), -163.01 – -163.30 (m) [Figure S23].

Table S1 Crystallographic data

Empirical formula	C_{64} H_{41} Co F_{10} N_4 O_2 P	$C_{43}H_{19}F_{10}FeN_5O_3$
Fw	1177.91	899.48
Radiation	MoKα (λ = 0.71073)	CuKα (λ = 1.54184)
Crystal symmetry	Monoclinic	Monoclinic
Space group	$P2_1/c$	Pn
a(Å)	8.609 (3)	8.1606 (3)
b(Å)	25.25 (3)	40.3164 (8)
c(Å)	25.400 (12)	11.4724 (4)
α(deg)	90.00	90
β(deg)	105.318 (12)	106.081 (3)
γ(deg)	90.00	90
$V(Å^3)$	5324 (7)	3626.8 (2)
Z	4	4
μ (mm^{-1})	0.439	4.261
T (K)	200	100
D_{calcd} (g cm^{-3})	1.469	1.647
2θ range (deg)	2.32 to 48.28	8.316 to 136.502
e data (R_{int})	7813 (0.0920)	11257 (0.0557)
R1 ($I>2\sigma(I)$)	0.0944 (6781)	0.0528 (9860)
WR2 (all data)	0.1952 (7813)	0.1434 (11257)
GOF	1.348	1.083
CCDC	1913981	1913983

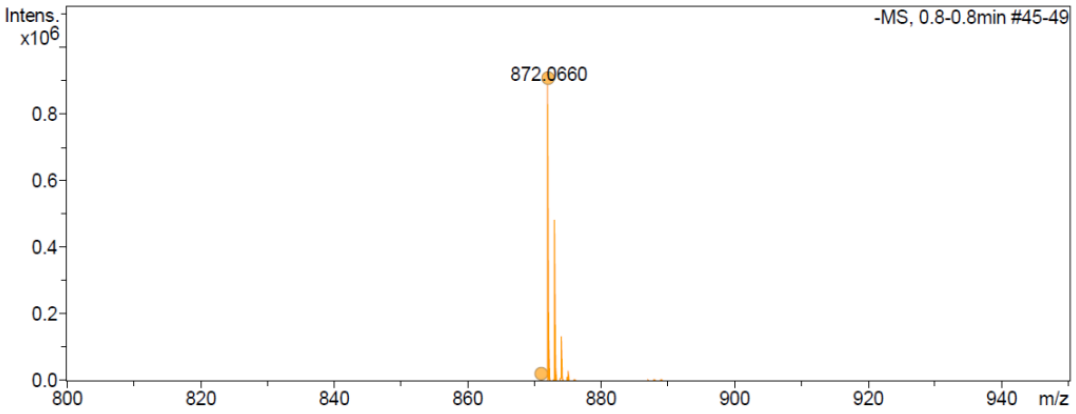

Meas. m/z	#	Ion Formula	m/z	err [ppm]	mSigma	# mSigma	Score	rdb	e⁻ Conf	N-Rule	|err| [mDa]
871.0474	1	C43H18CoF10N4O2	871.0608	15.4	605.1	1	100.00	32.0	odd	-	13.4
	1	C43H18CoF10N4O2	871.0608	15.4	605.1	1	100.00	32.0	odd	-	13.4
872.0660	1	C43H19CoF10N4O2	872.0686	3.0	36.1	1	100.00	31.5	even	-	2.6

Figure S1. HRMS spectrum of **1-Co(PPh$_3$)** [M -PPh$_3$]$^-$.

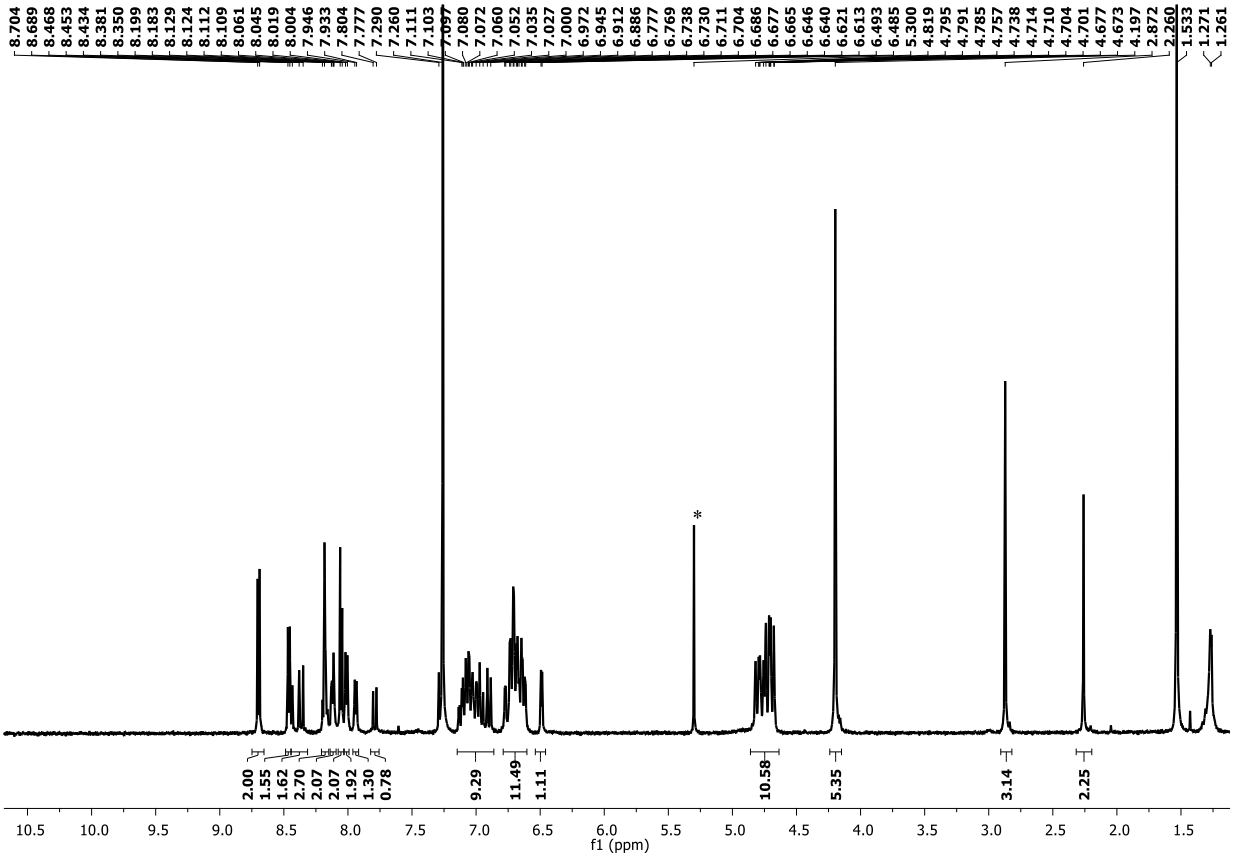

Figure S2. ^{1}H NMR spectrum of **1-Co(PPh$_3$)** in $CDCl_3$ (300 MHz).

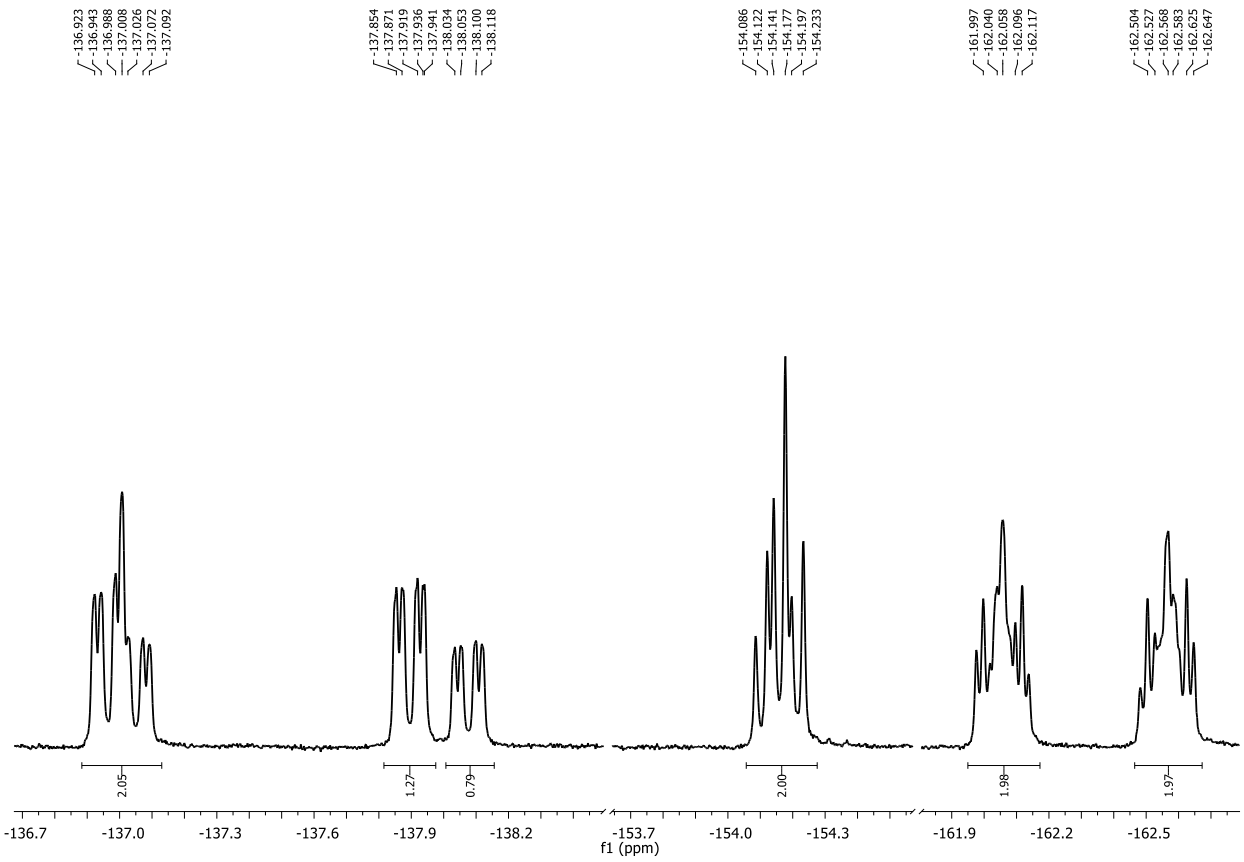

Figure S3. ^{19}F NMR spectrum of **1-Co(PPh$_3$)** in $CDCl_3$ (377 MHz).

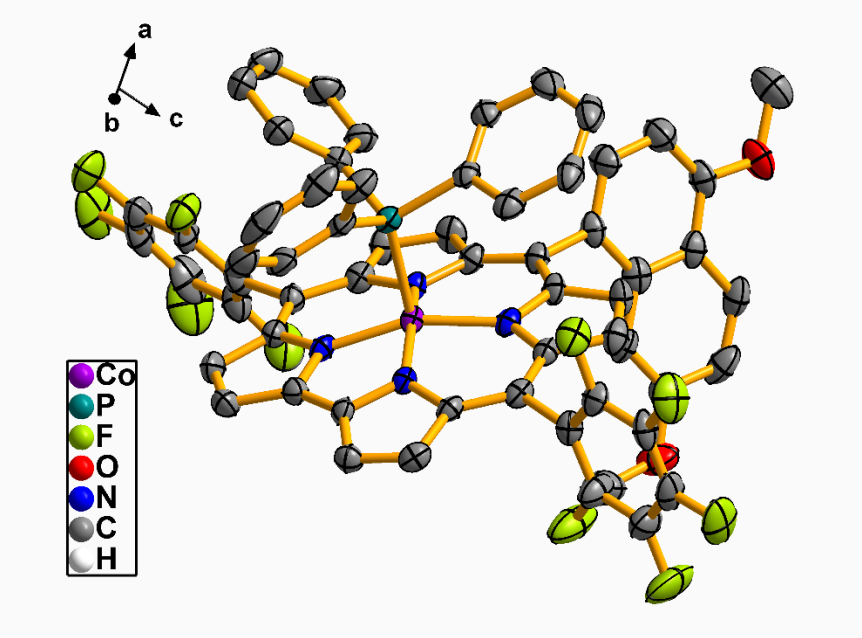

Figure S4. ORTEP representation of the crystal structure of **1-Co(PPh$_3$)**. Ellipsoids are drawn at 50% probability.

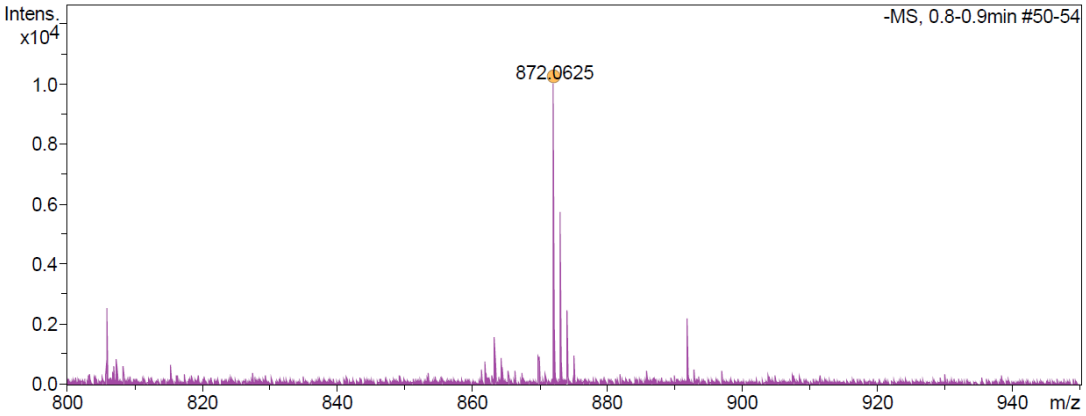

Meas. m/z	#	Ion Formula	m/z	err [ppm]	mSigma	#	mSigma	Score	rdb	e¯	Conf	N-Rule	|err| [mDa]	|err| [mDa]
872.0625	1	C43H19CoF10N4O2	872.0686	7.0	75.7	1	100.00	31.5	even			-	6.1	6.1

Figure S5. HRMS spectrum of **1-Co(Py)$_2$** [M -Py$_2$]$^-$.

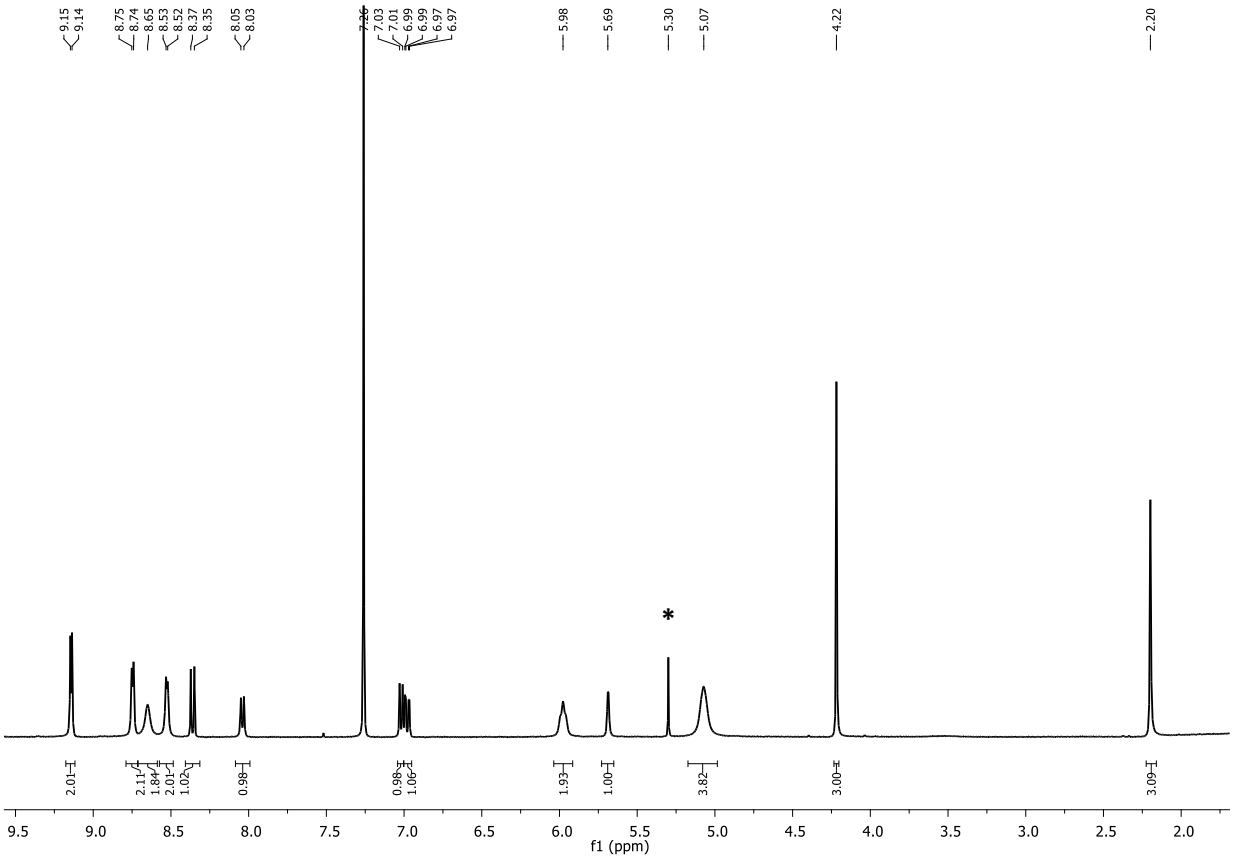

Figure S6. ^{1}H NMR spectrum of **1-Co(Py)$_2$** in $CDCl_3$ (400 MHz).

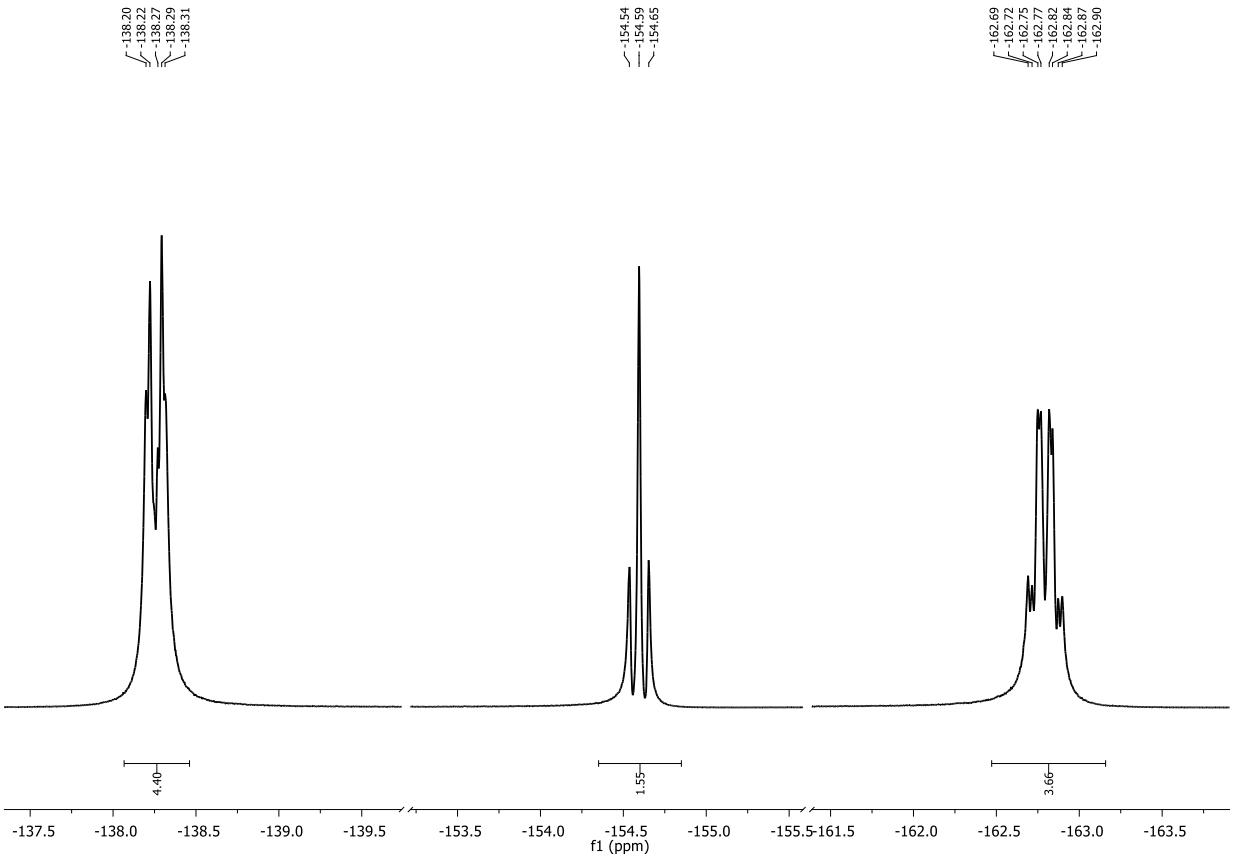

Figure S7. ^{19}F NMR spectrum of **1-Co(Py)$_2$** in $CDCl_3$ (377 MHz).

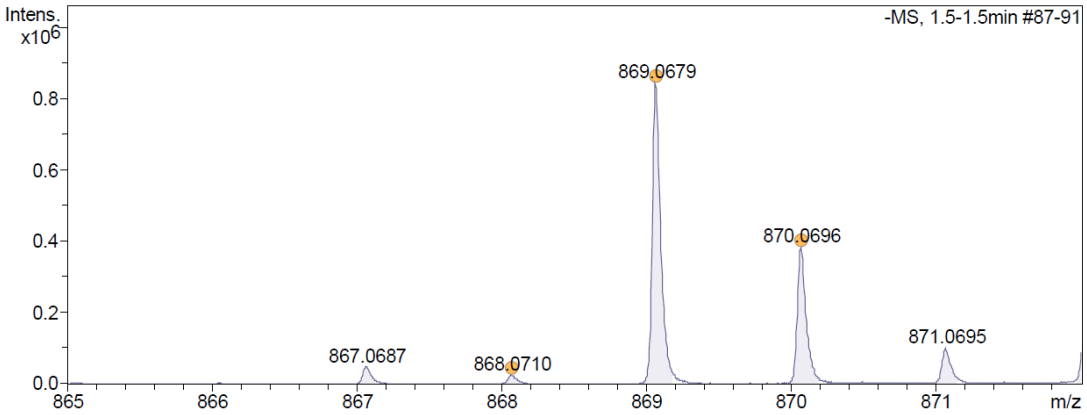

Meas. m/z	#	Ion Formula	m/z	err [ppm]	mSigma	# mSigma	Score	rdb	e¯ Conf	N-Rule	|err| [mDa]
868.0710	1	C43H18F10FeN4O2	868.0625	-9.6	466.3	1	100.00	32.0	odd	ok	8.4
	1	C43H18F10FeN4O2	868.0625	-9.6	466.3	1	100.00	32.0	odd	ok	8.4
869.0679	1	C43H19F10FeN4O2	869.0703	2.9	531.9	1	100.00	31.5	even	ok	2.5
	1	C43H19F10FeN4O2	869.0703	2.9	531.9	1	100.00	31.5	even	ok	2.5
870.0696	1	C43H20F10FeN4O2	870.0781	10.0	623.7	1	100.00	31.0	odd	ok	8.7
	1	C43H20F10FeN4O2	870.0781	10.0	623.7	1	100.00	31.0	odd	ok	8.7

Figure S8. HRMS spectrum of **1-Fe(NO)** $[M - NO]^-$.

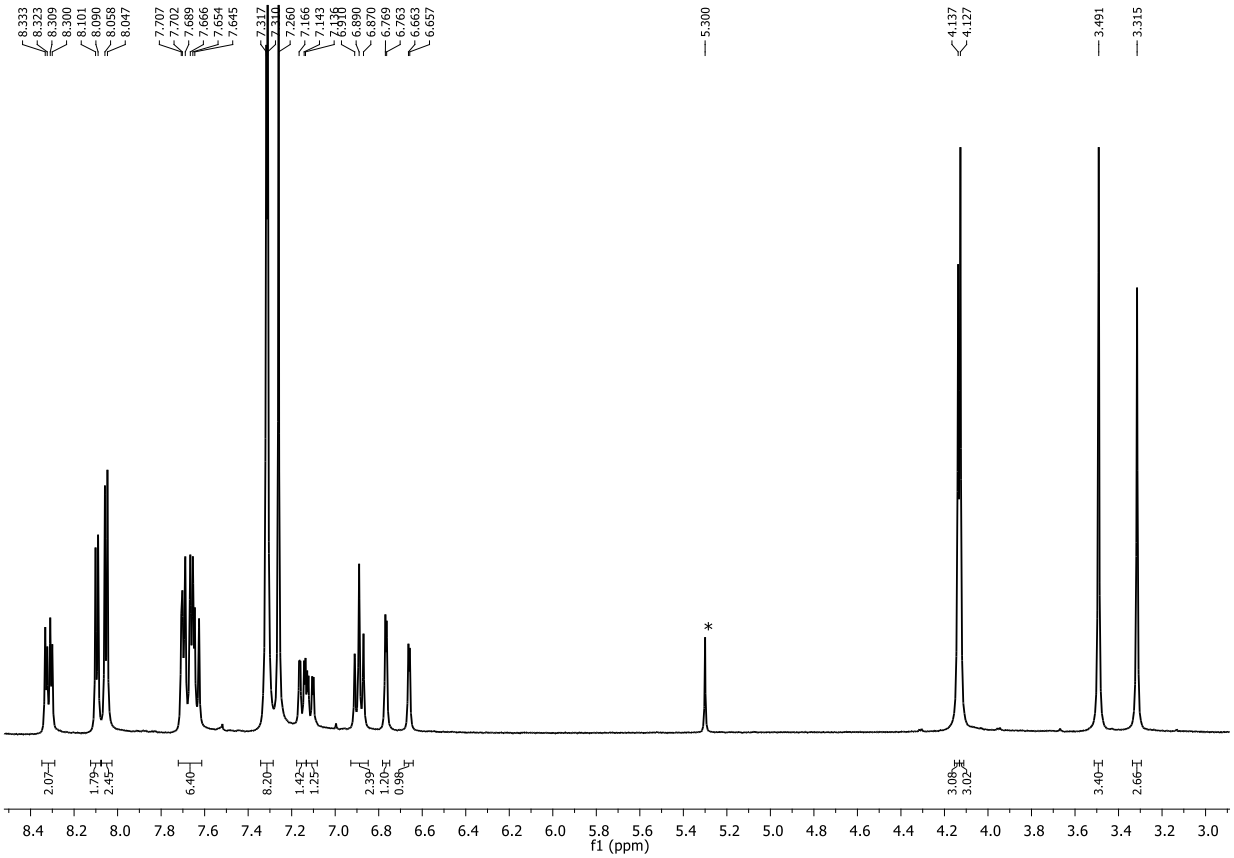

Figure S9. ^1H NMR spectrum of **1-Fe(NO)** in $CDCl_3$ (400 MHz).

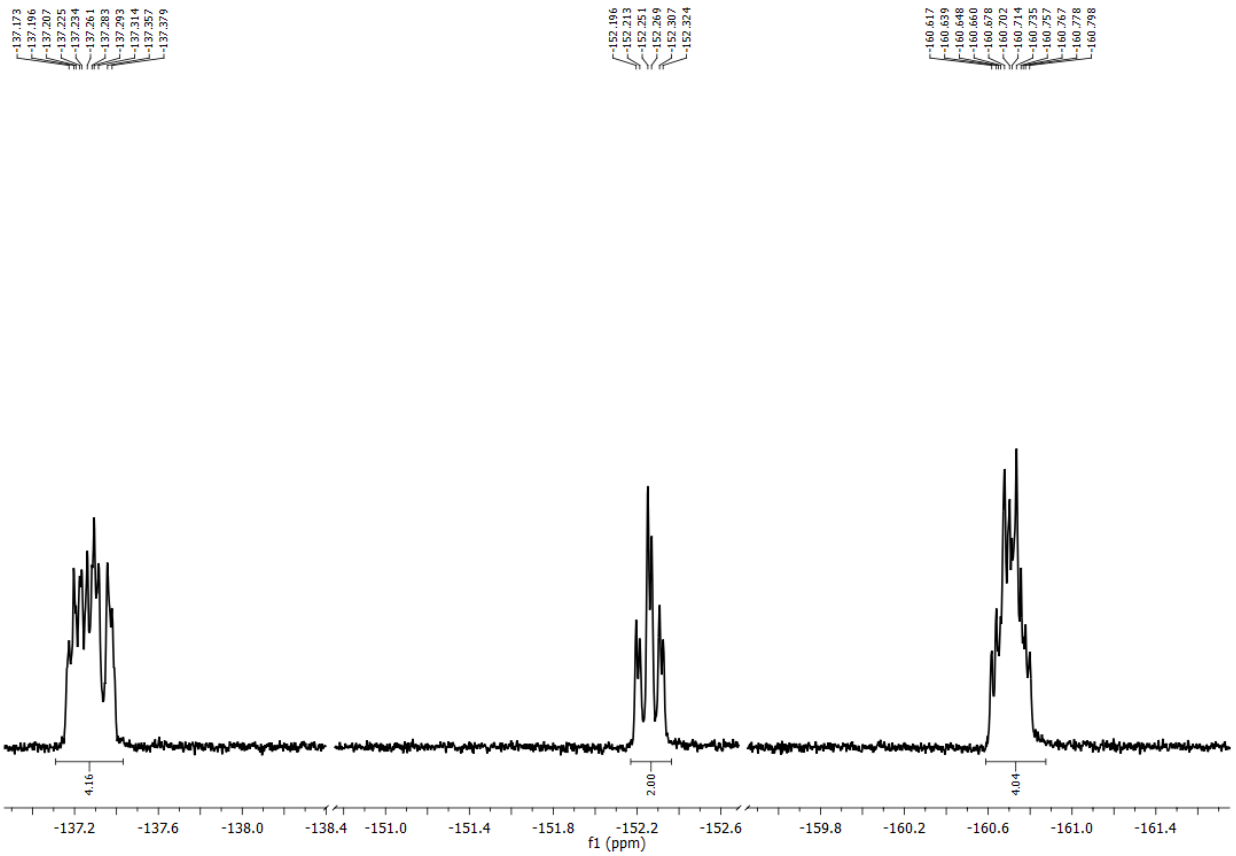

Figure S10. ^{19}F NMR spectrum of **1-Fe(NO)** in $CDCl_3$ (377 MHz).

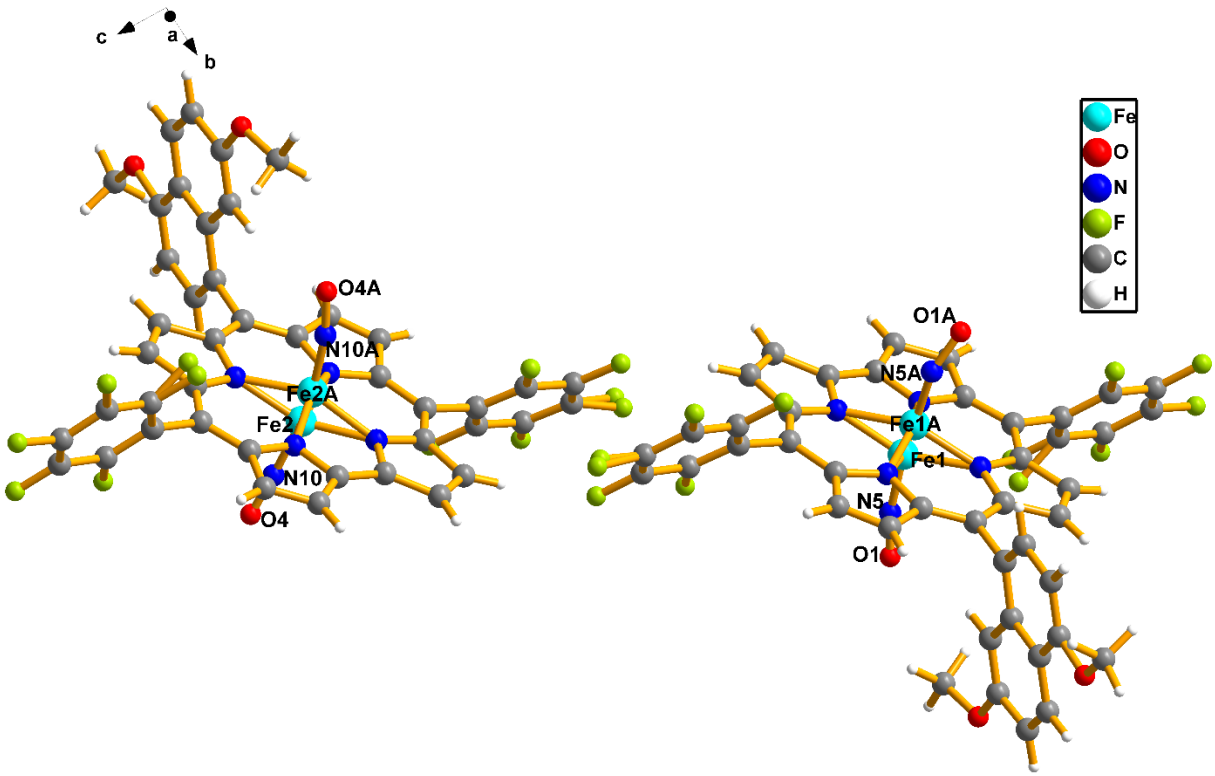

Figure S11. X-ray structure of **1-Fe(NO)** revealing the disordered iron nitrosyl centers. The structure contains two molecules in the asymmetric unit. The occupancies are refined. In one type of molecule Fe1-N5-O1 is 87.1% and Fe1A-N5A-O1A is 12.9%; in the other type, Fe2-N4-O10 is 68.4% and Fe2A-N4A-O10A is 31.6%.

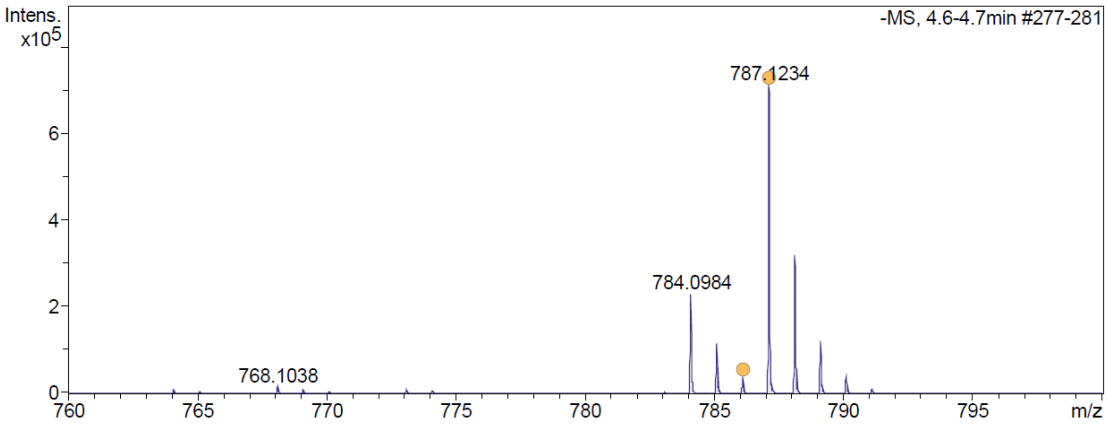

Meas. m/z	#	Ion Formula	m/z	err [ppm]	mSigma	# mSigma	Score	rdb	e⁻ Conf	N-Rule	|err| [mDa]
786.1073	1	C41H16F10N4O2	786.1119	5.9	575.0	1	100.00	31.0	odd	ok	4.6
787.1234	1	C41H17F10N4O2	787.1197	-4.7	34.5	1	100.00	30.5	even	ok	3.7

Figure S12. HRMS spectrum of **2** $[M-H]^-$.

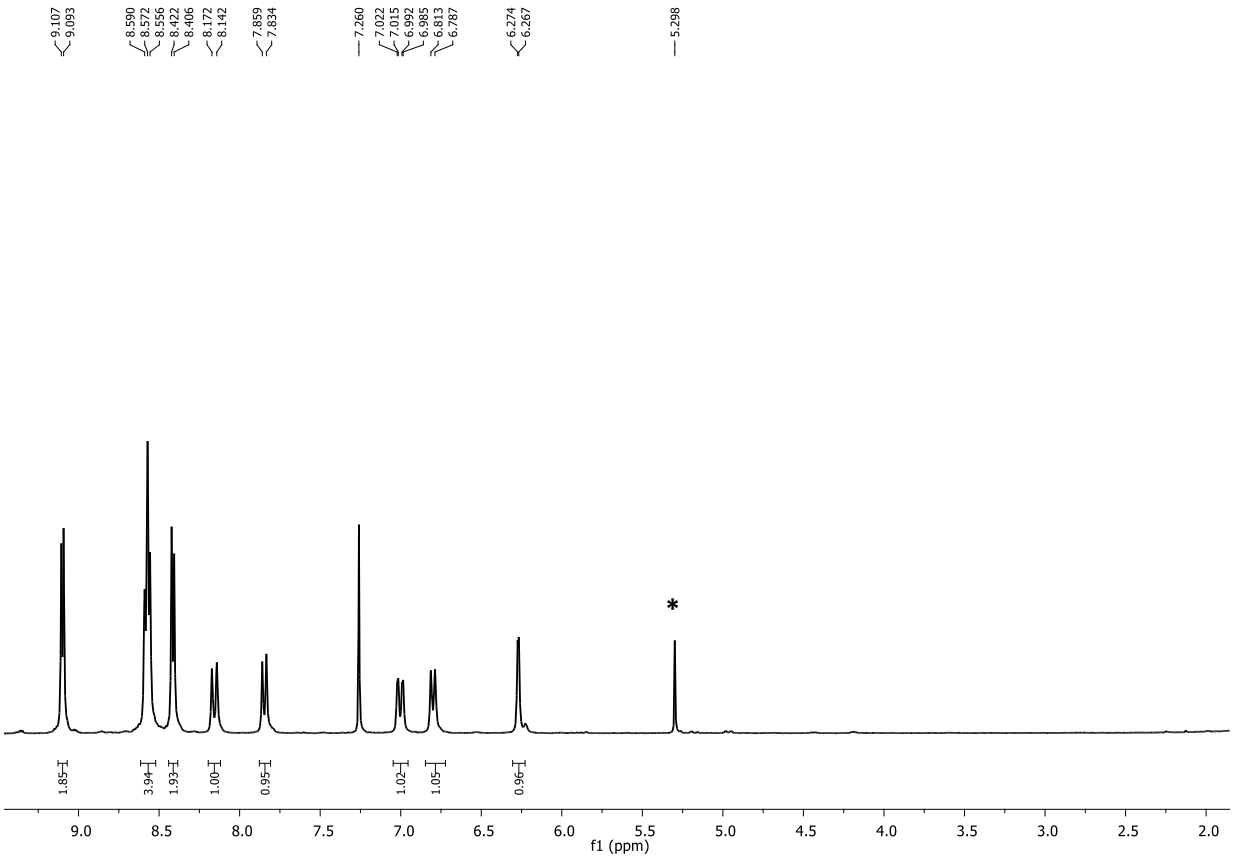

Figure S13. ^1H NMR spectrum of **2** in $CDCl_3$ (300 MHz).

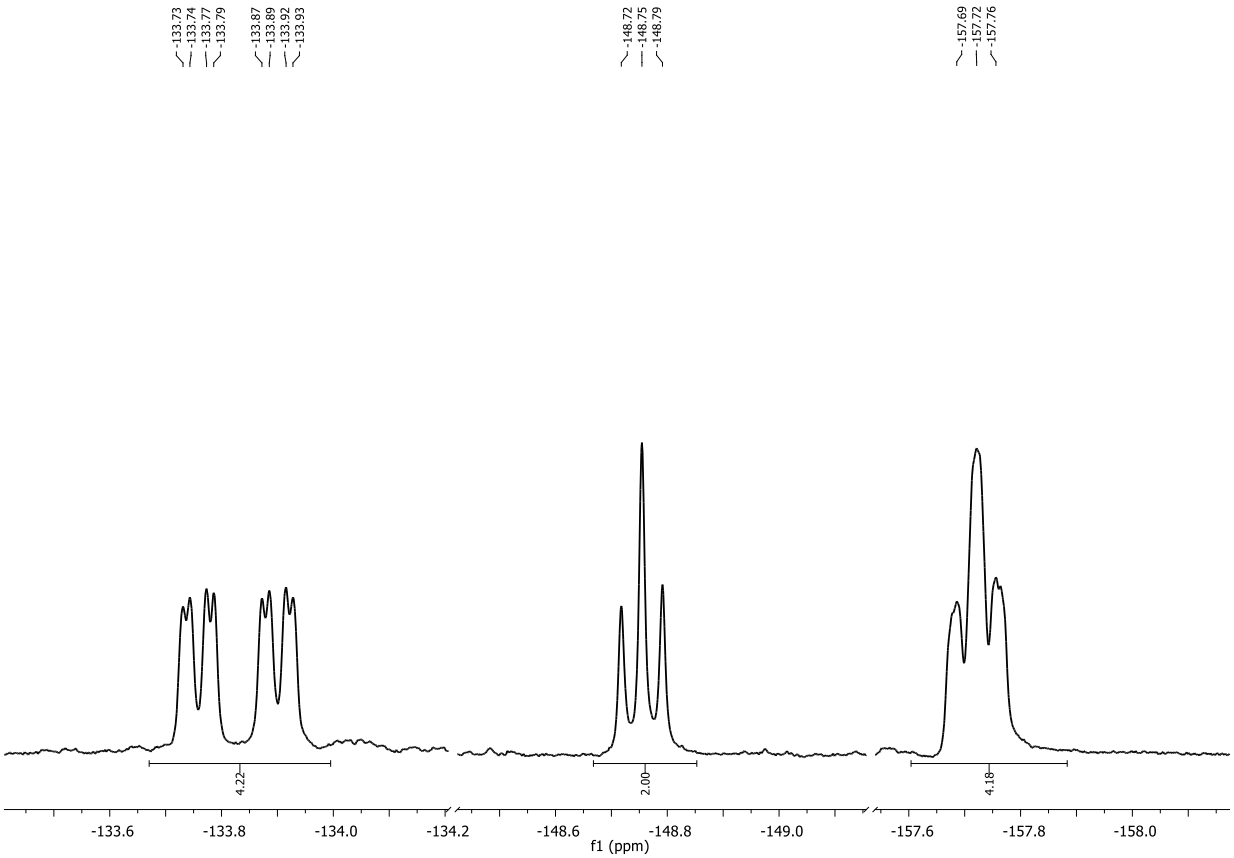

Figure S14. ^{19}F NMR spectrum of **2** in $CDCl_3$ (565 MHz).

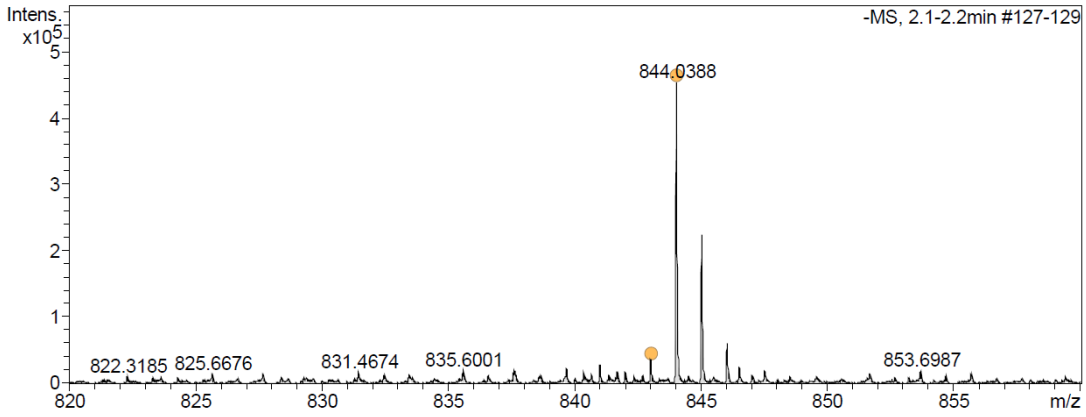

Meas. m/z	#	Ion Formula	m/z	err [ppm]	mSigma	# mSigma	Score	rdb	e⁻ Conf	N-Rule	|err| [mDa]
843.0294	1	C41H14CoF10N4O2	843.0295	0.1	571.8	1	100.00	32.0	odd	-	0.1
	1	C41H14CoF10N4O2	843.0295	0.1	571.8	1	100.00	32.0	odd	-	0.1
844.0388	1	C41H15CoF10N4O2	844.0373	-1.8	22.5	1	100.00	31.5	even	-	1.5

Figure S15. HRMS spectrum of **2-Co(Py)$_2$** [M -Py_2]$^-$.

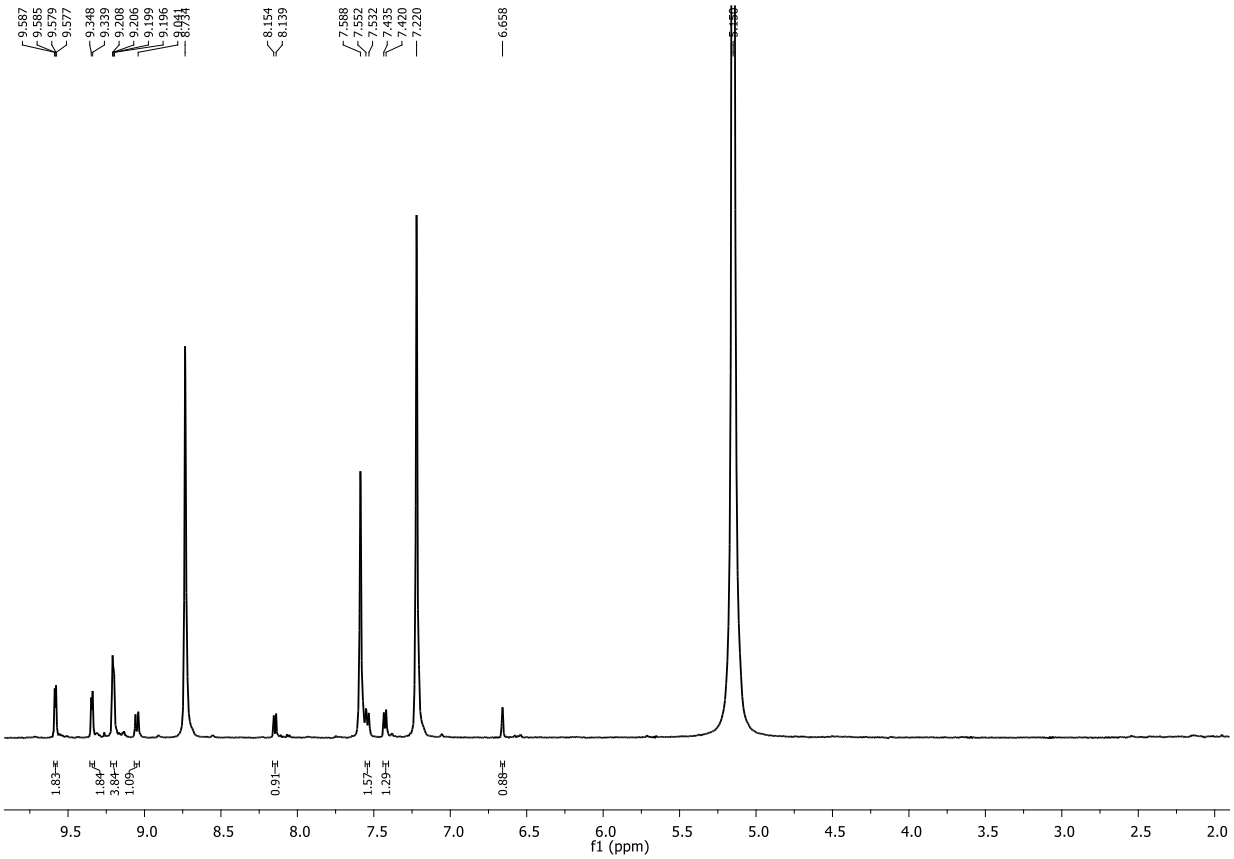

Figure S16. ^{1}H NMR spectrum of **2-Co(Py)$_2$** in pyridine-d$_5$ (500 MHz).

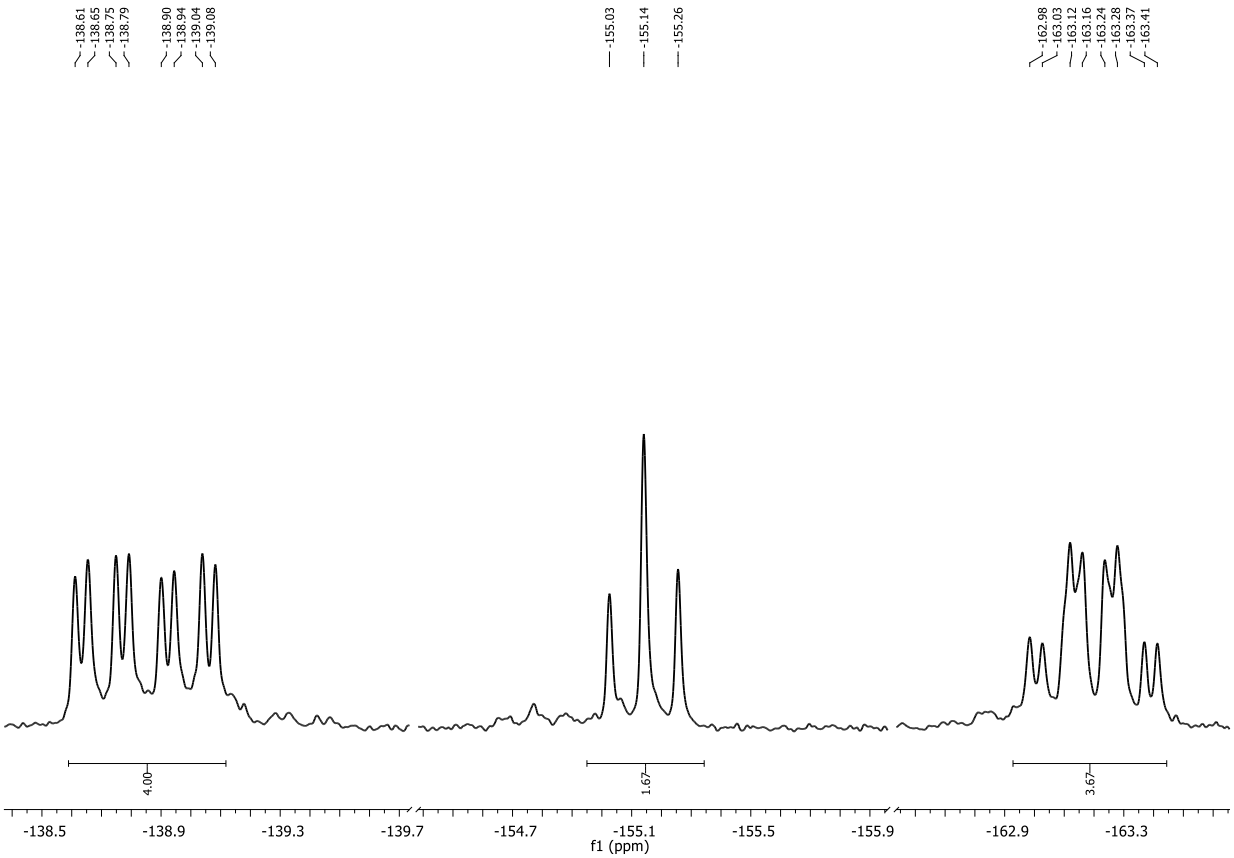

Figure S17. ^{19}F NMR spectrum of **2-Co(Py)$_2$** in pyridine-d$_5$ (188.31 MHz).

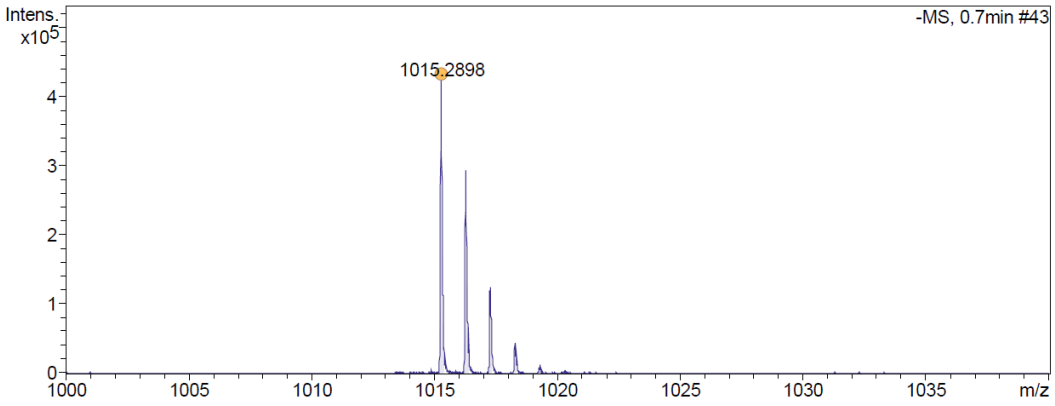

Meas. m/z	#	Ion Formula	m/z	err [ppm]	mSigma	# mSigma	Score	rdb	e¯ Conf	N-Rule	|err| [mDa]
1015.2898	1	C53H45F10N4O2Si2	1015.2927	2.8	7.1	1	100.00	30.5	even	ok	2.9

Figure S18. HRMS spectrum of **3** [M -H]$^-$.

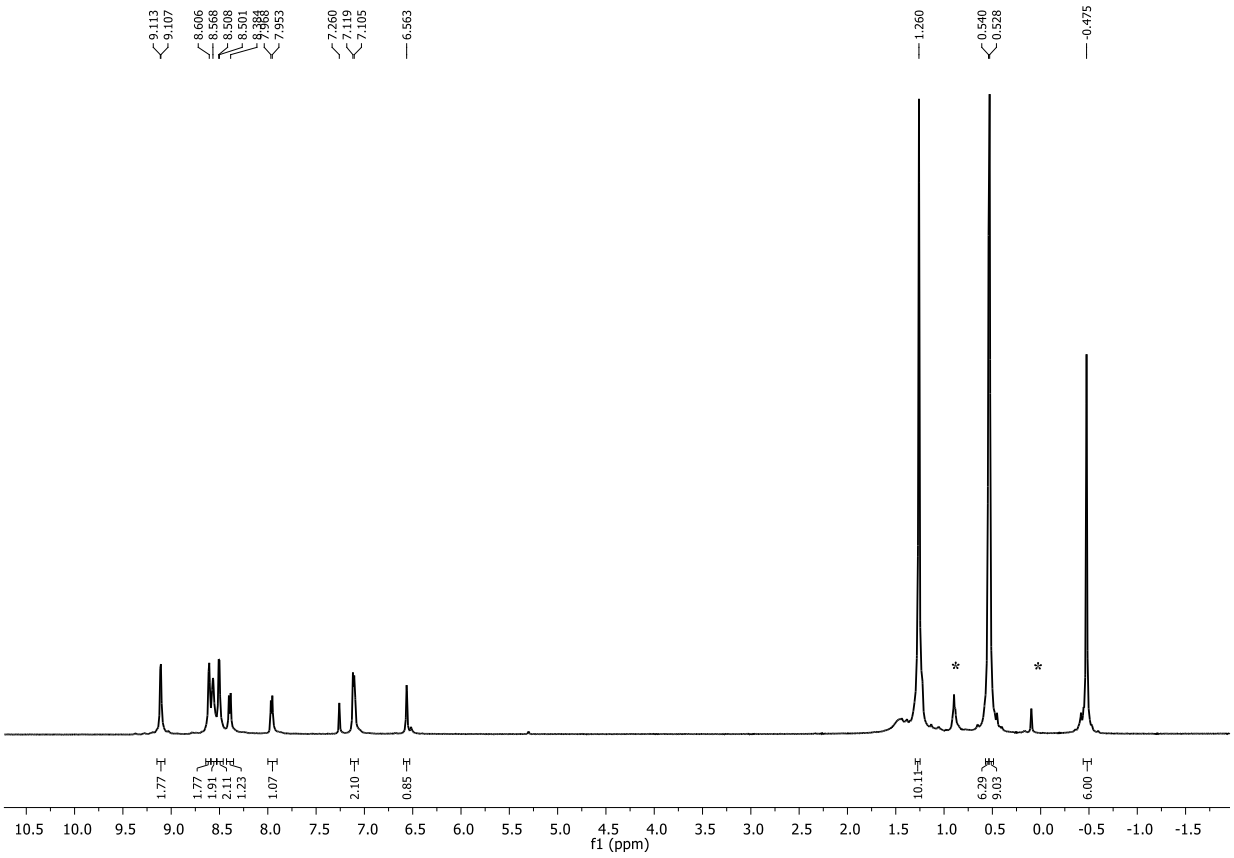

Figure S19. ^{1}H NMR spectrum of **3** in $CDCl_3$ (500 MHz).

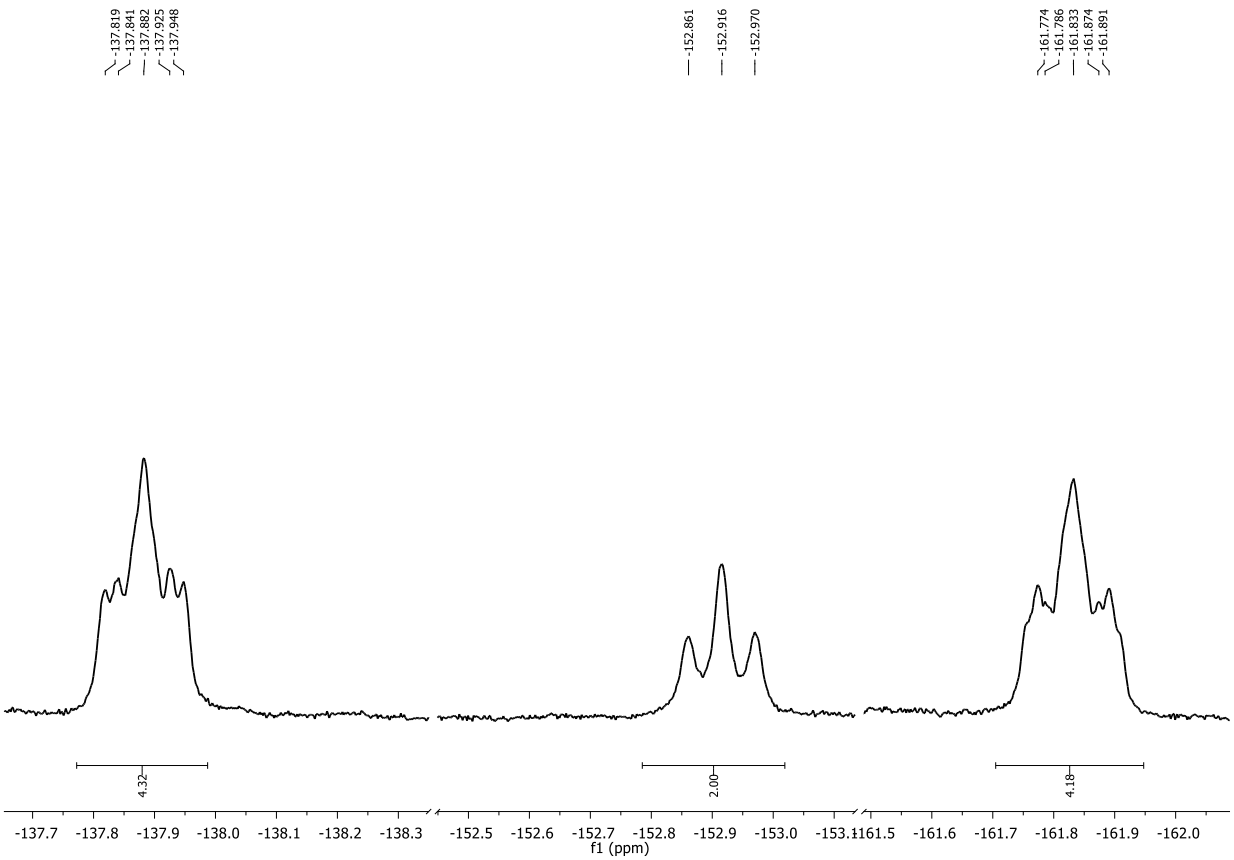

Figure S20. ^{19}F NMR spectrum of **3** in $CDCl_3$ (377 MHz).

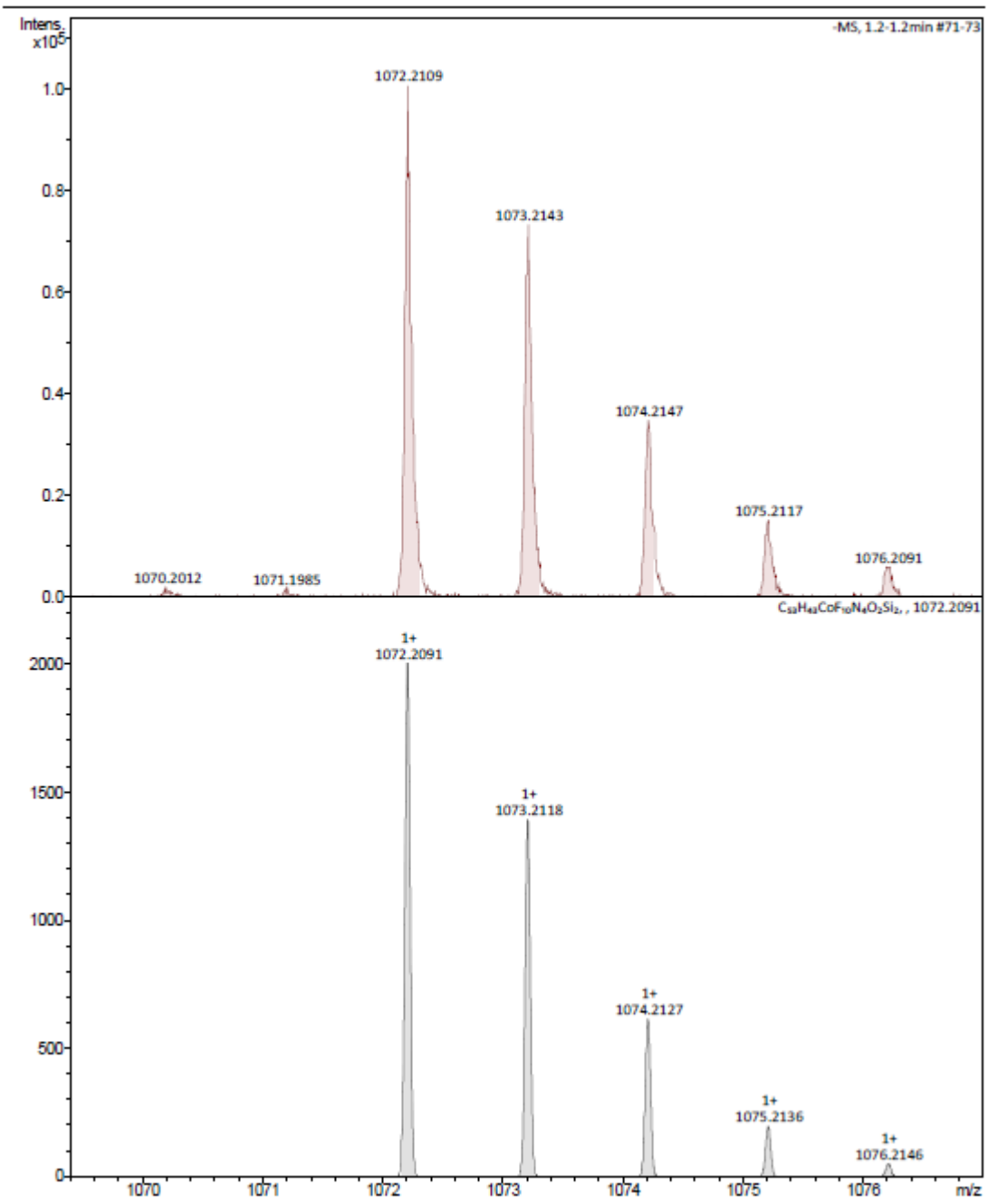

Figure S21. HRMS spectrum of **3-Co(Py)$_2$** [M -Py$_2$]$^-$.

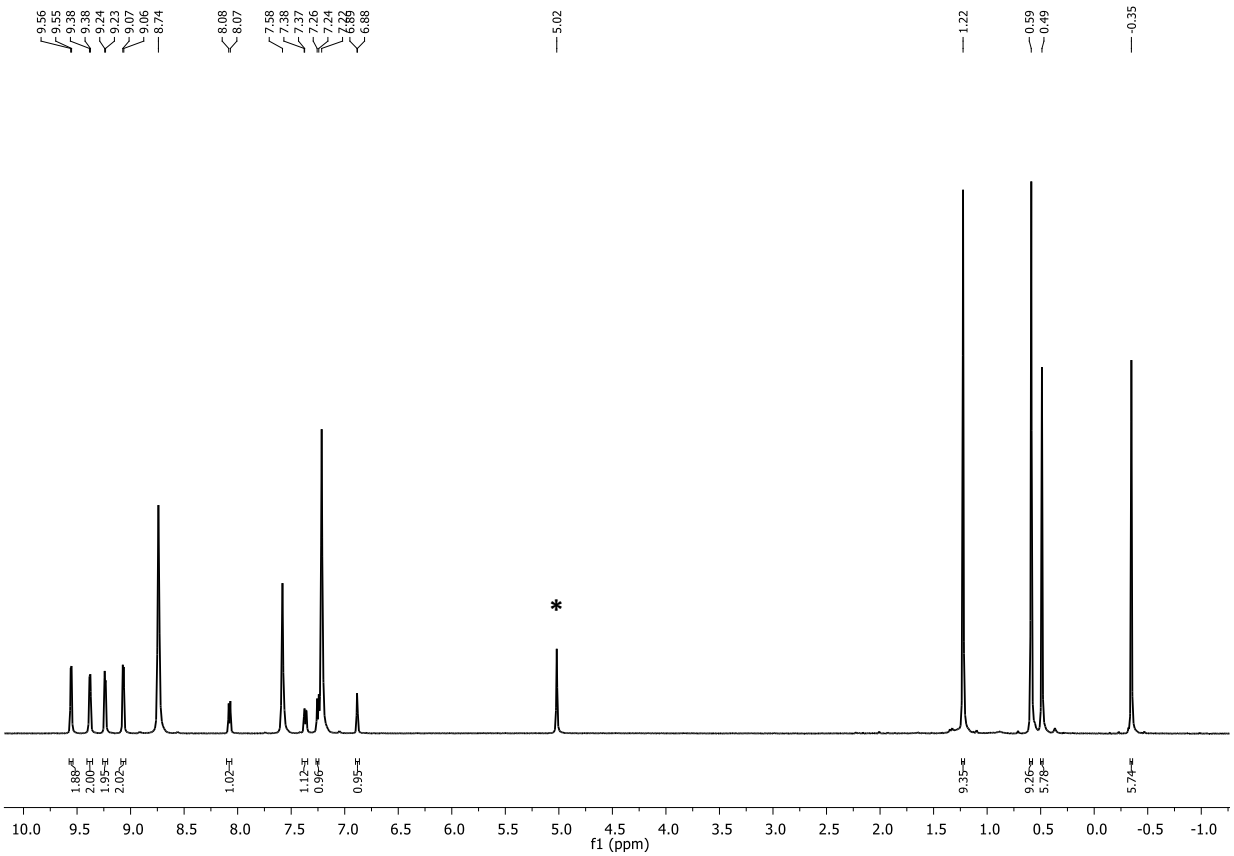

Figure S22. ^{1}H NMR spectrum of **3-Co(Py)$_2$** in pyridine-d$_5$ (500 MHz).

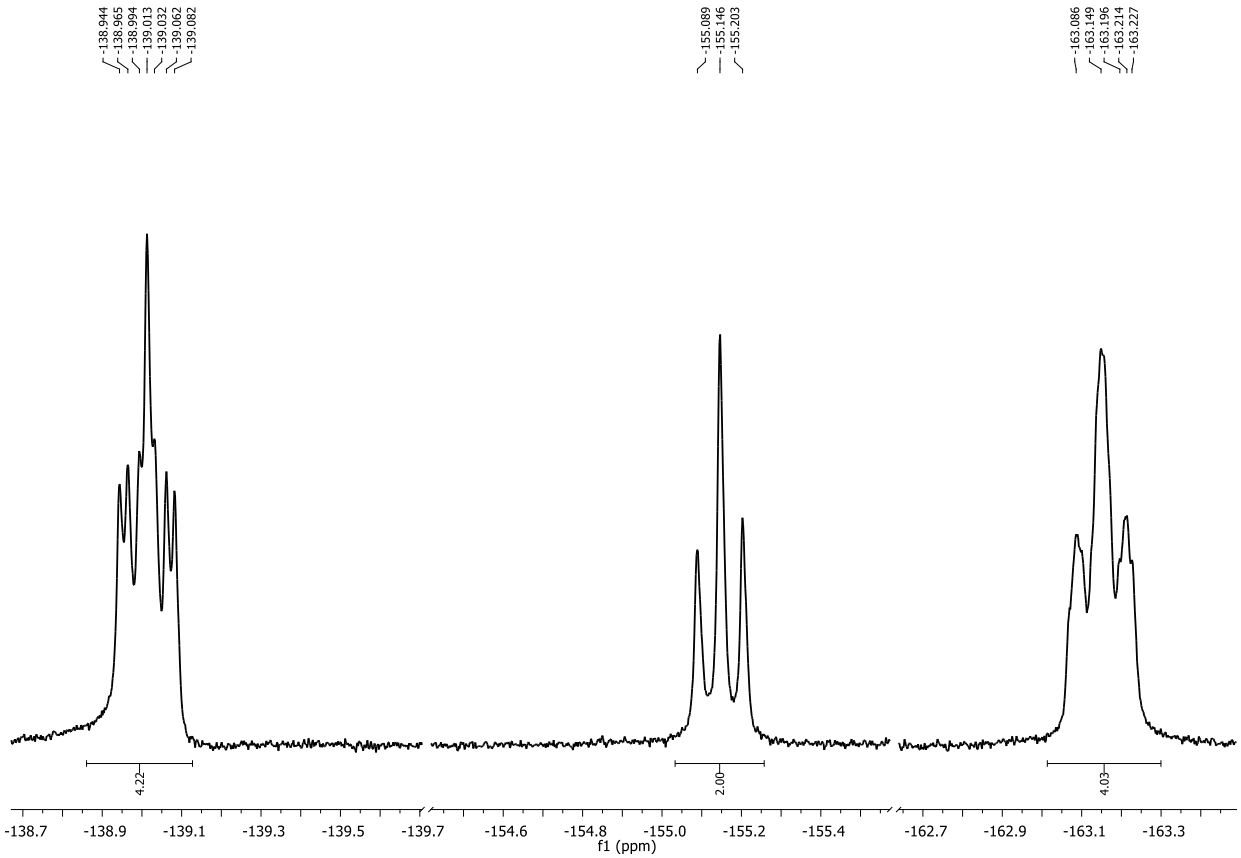

Figure S23. ^{19}F NMR spectrum of **3-Co(Py)$_2$** in pyridine-d$_5$ (377 MHz).

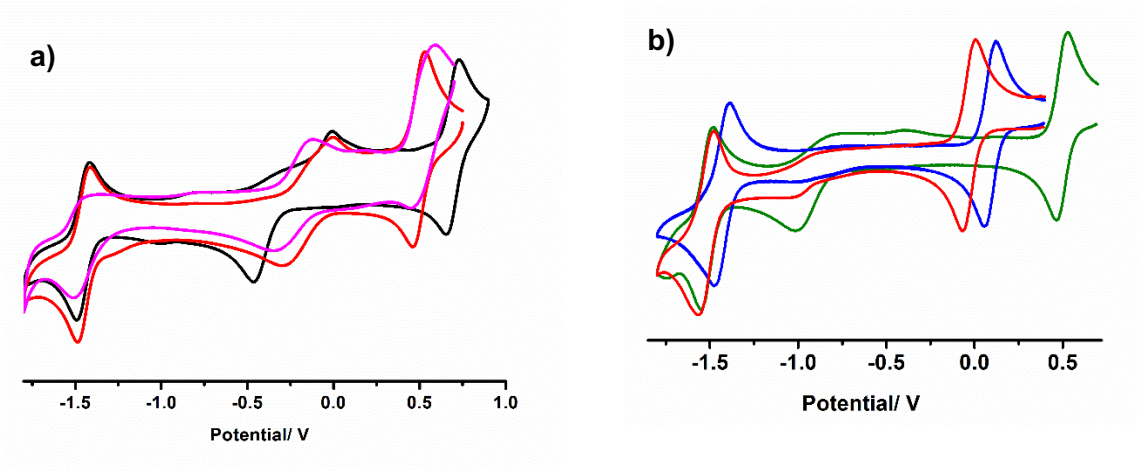

Figure S24. Cyclic voltammetric patterns of 0.5 mM acetonitrile solutions of (a) **1-Co(PPh$_3$)** (black), **1-Co(Py)$_2$** (red) and **2-Co(Py)$_2$** (pink) and (b) **1-Fe(NO)** (red), **tpfc-Fe(NO)** (blue) and **tpfc-Fe(Cl)** (green) in presence of 0.1 M TBAP.

Table S2. Electrochemical data (0.5 mM metallocorrole, 0.1 M TBAP, scan rates of 0.1V/s) with potentials listed vs. Ag/AgCl[a]

Compound Name	Redox Potentials (V)
1-Co(PPh$_3$)[b]	0.69, -1.45
1-Co(Py)$_2$ [b]	0.50, -1.44
2-Co(Py)$_2$ [b]	0.52, -1.48
1-Fe(NO)	0.03, -1.52
tpfc-Fe(NO)	0.09, -1.43
tpfc-Fe(Cl) [c]	0.49, -1.52

(a) The potential recorded for the Fc/Fc$^+$ couple in CH$_3$CN was 0.45 V.

(b) The redox potentials of the Co $^{II/III}$ couples are not listed due to their irreversible nature.

(c) The redox potentials of the Fe $^{II/III}$ couple is not listed due to its irreversible nature.

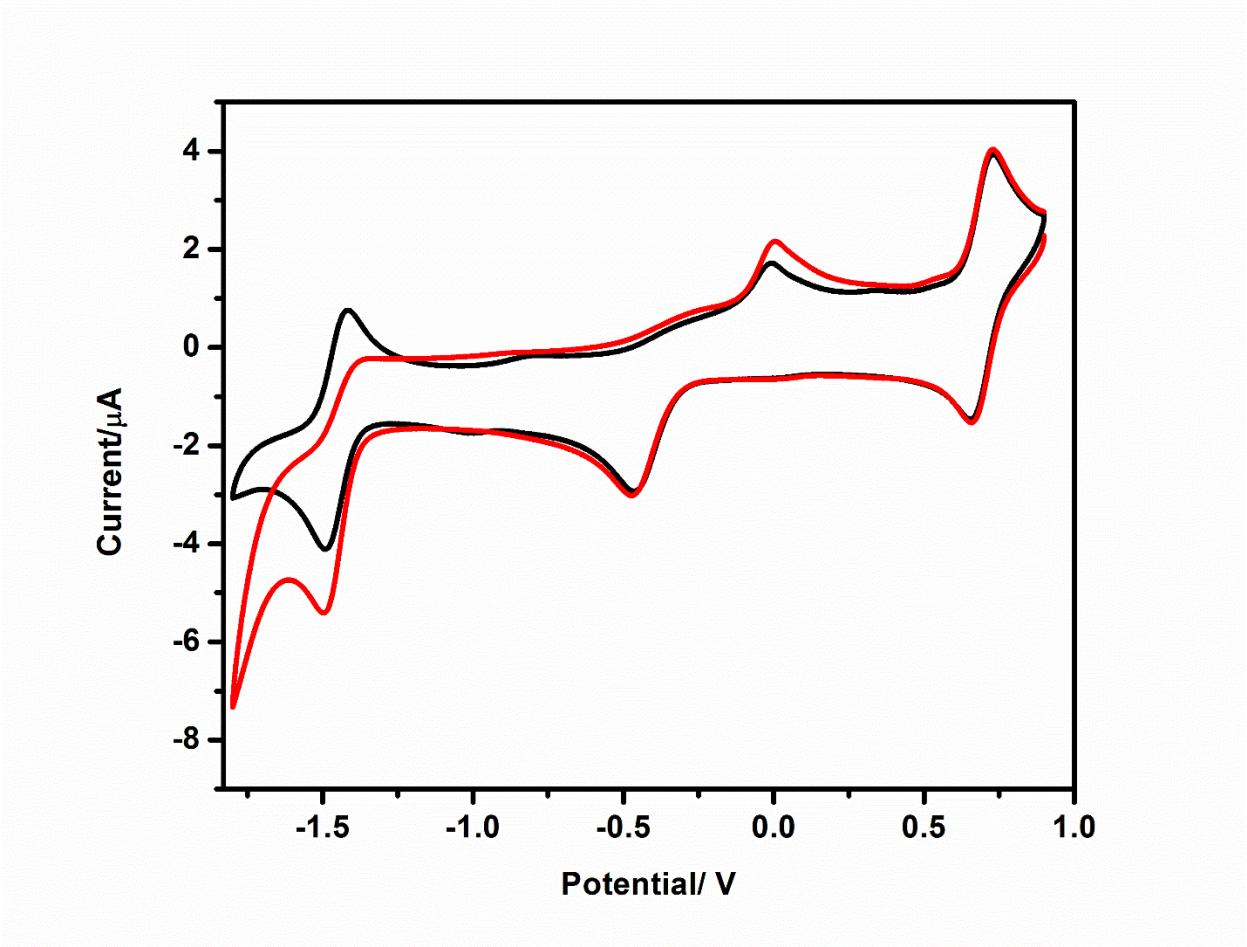

Figure S25. Cyclic voltammograms of acetonitrile solution of 0.5 mM **1-CoPPh$_3$** in the presence of argon (black) and carbon dioxide (red) respectively. The potentials are vs. Ag/AgCl.

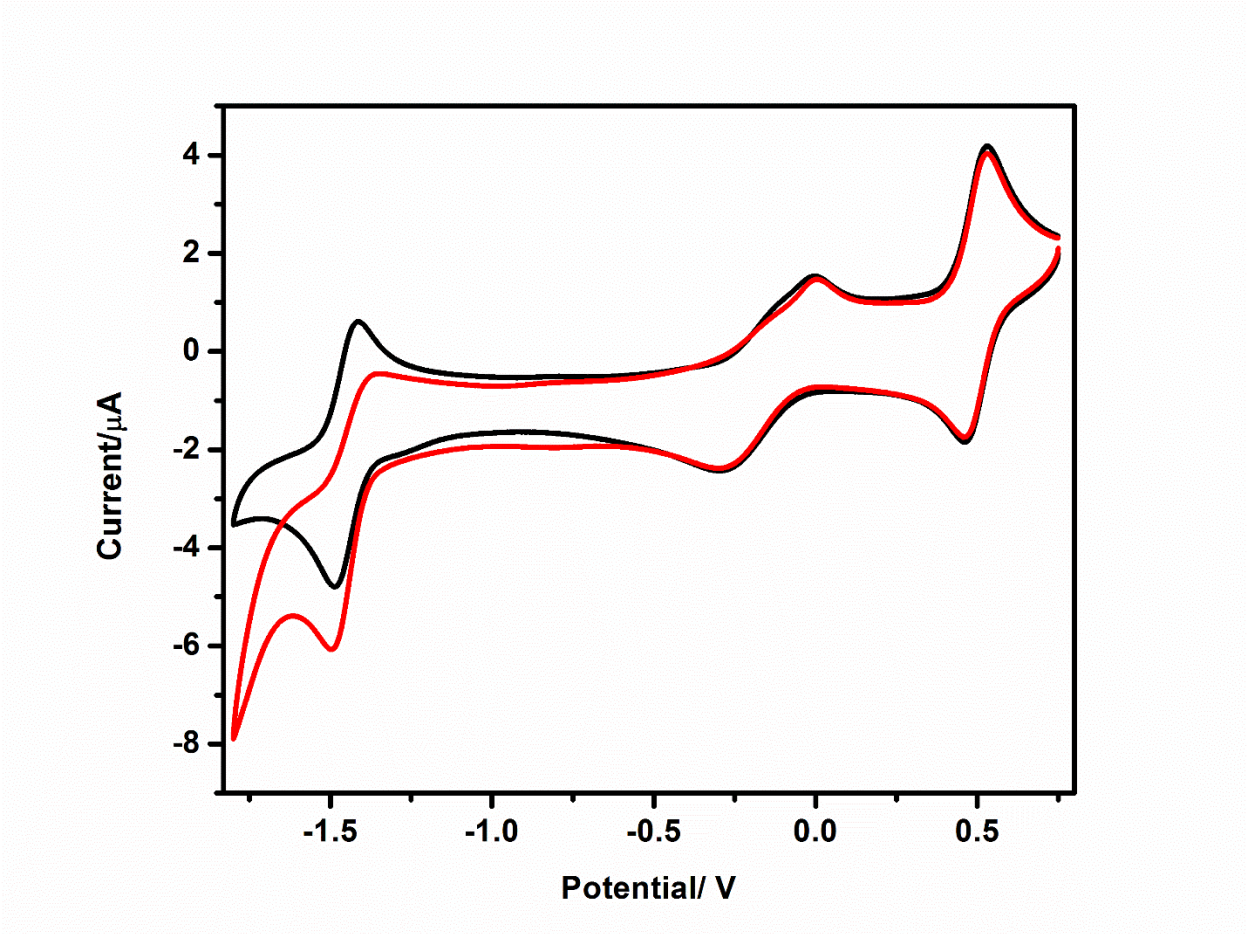

Figure S26. Cyclic voltammograms of acetonitrile solution of 0.5 mM **1-CoPy$_2$** in the presence of argon (black) and carbon dioxide (red) respectively. The potentials are vs. Ag/AgCl.

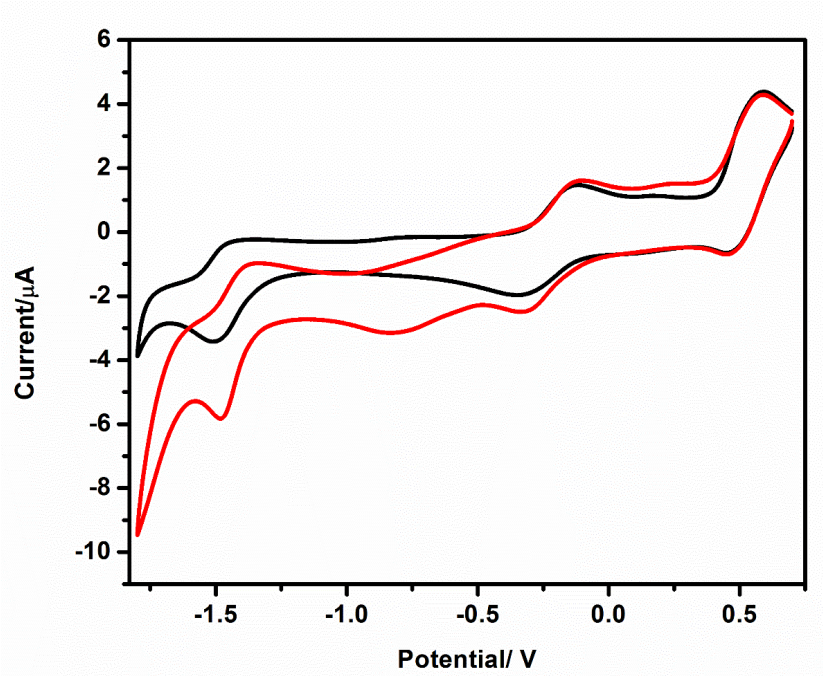

Figure S27. Cyclic voltammograms of acetonitrile solution of 0.5 mM **2-CoPy$_2$** in the presence of argon (black) and carbon dioxide (red) respectively. The potentials are vs. Ag/AgCl.

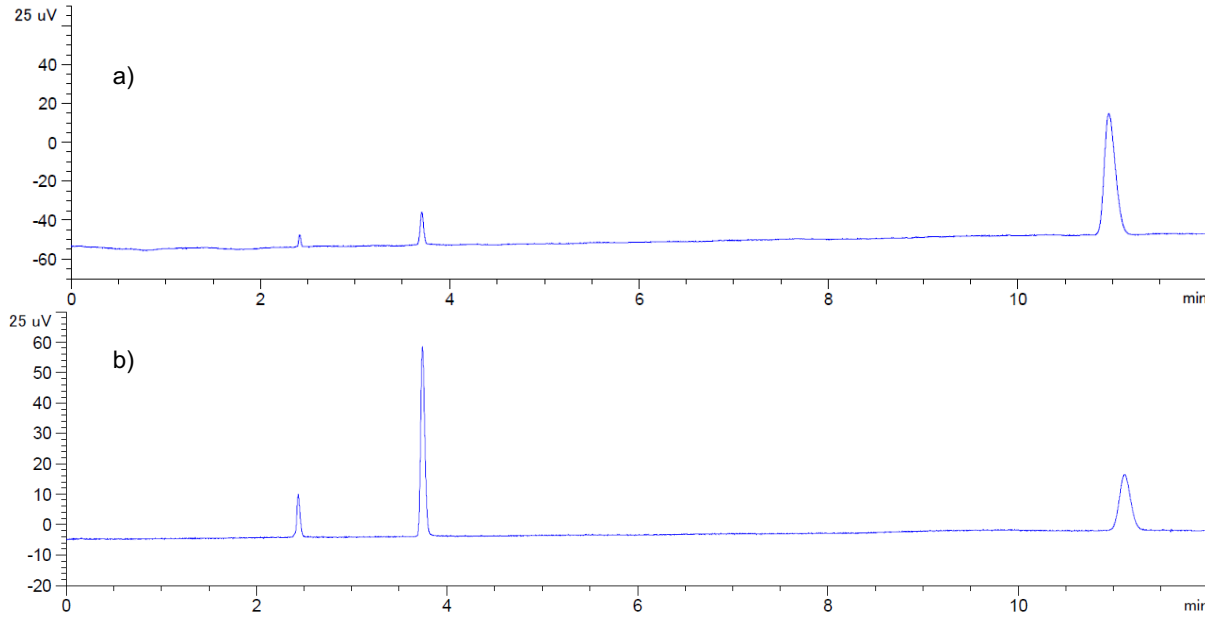

Figure S28. Gas chromatography plots displaying the signals corresponding to (a) a pure CO sample with retention time of 11 min and (b) that corresponding to a headspace gas mixture after 2 hours of bulk electrolysis of a solution containing **1-Fe(NO)** as the catalyst.

References

1. D. Kappa CCD Server Software; Nonius BV, T. N., **1997**.
2. Otwinowski, Z.; Minor, W., [20] Processing of X-ray diffraction data collected in oscillation mode. In *Methods Enzymol.*, Elsevier: 1997; Vol. 276, pp 307-326.
3. Dolomanov, O. V.; Bourhis, L. J.; Gildea, R. J.; Howard, J. A. K.; Puschmann, H., OLEX2: a complete structure solution, refinement and analysis program. *J. Appl. Crystallogr.* **2009,** *42* (2), 339-341.
4. Burla, M. C.; Caliandro, R.; Camalli, M.; Carrozzini, B.; Cascarano, G. L.; De Caro, L.; Giacovazzo, C.; Polidori, G.; Siliqi, D.; Spagna, R., IL MILIONE: a suite of computer programs for crystal structure solution of proteins. *J. Appl. Crystallogr.* **2007,** *40* (3), 609-613.
5. Sheldrick, G., Crystal structure refinement with SHELXL. *Acta Cryst. C* **2015,** *71* (1), 3-8.
6. CrysAlis^{PRO} – Rigaku.
7. Sheldrick, G. M. SHELXT - Integrated Space-Group and Crystal-Structure Determination. *Acta Crystallogr., Sect. A: Fundam. Crystallogr.* **2015**, *71*, 3-8.
8. Mahammed, A.; Giladi, I.; Goldberg, I.; Gross, Z., Synthesis and Structural Characterization of a Novel Covalently-Bound Corrole Dimer. *Chem. Eur. J.* **2001,** *7* (19), 4259-4265.
9. (a) Sinha, W.; Deibel, N.; Agarwala, H.; Garai, A.; Schweinfurth, D.; Purohit, C. S.; Lahiri, G. K.; Sarkar, B.; Kar, S., Synthesis, Spectral Characterization, Structures, and Oxidation State Distributions in [(corrolato)FeIII(NO)]n (n = 0, +1, −1) Complexes. *Inorg. Chem.* **2014,** *53* (3), 1417-1429; (b) Autret, M.; Will, S.; Caemelbecke, E. V.; Lex, J.; Gisselbrecht, J.-P.; Gross, M.; Vogel, E.; Kadish, K. M., Synthesis and Electrochemistry of Iron(III) Corroles Containing a Nitrosyl Axial Ligand. Spectral Characterization of [(OEC)FeIII(NO)]n where n = 0, 1, 2, or -1 and OEC is the Trianion of 2,3,7,8,12,13,17,18-Octaethylcorrole. *J. Am. Chem. Soc.* **1994,** *116* (20), 9141-9149.